# Local structure in $\beta$-$Ti_{1-y}V_yH_x$ studied by inelastic neutron scattering

Takahiro Ueda and Shigenobu Hayashi
*Department of Physical Chemistry, National Institute of Materials and Chemical Research, Tsukuba, Ibaraki 305, Japan*

Yusuke Nakai
*Institute of Materials Science, University of Tsukuba, Tsukuba, Ibaraki 305, Japan*

Susumu Ikeda
*National Laboratory for High Energy Physics, Tsukuba, Ibaraki 305, Japan*
(Received 17 May 1994; revised manuscript received 6 September 1994)

The hydrogen sites in the disordered metal hydrides, $\beta$-$Ti_{1-y}V_yH_x$ ($x\sim1$ and $0.2\le y\le0.9$) were studied using the incoherent inelastic neutron scattering (IINS) technique. The IINS spectra of the hydrides were collected at 50 K. Four peaks originated from the $\beta$ phase, whose energy ranges were $13\le\varepsilon\le16$ meV, $36\le\varepsilon\le44$ meV, $97\le\varepsilon\le110$ meV, and $134\le\varepsilon\le152$ meV. These peaks were assigned to the metal lattice vibrations and the local vibrational modes of hydrogen atoms occupying the octahedral site ($O$ site) and two kinds of tetrahedral sites ($T_1$ and $T_2$ sites), respectively. The ratio of the number of $T_1$ sites that were observed at the highest energy range to total hydrogen sites decreased and that of the $O$ site increased with increasing V content in the alloy. The composition dependence of the site fraction was analyzed using the cluster model modified to allow short-range ordering of metal atoms. The short-range order parameter was determined to be $0.43\pm0.05$.

## I. INTRODUCTION

Alloys composed of Ti and V, $Ti_{1-y}V_y$, are known to form compounds with hydrogen.[1,2] These alloys can absorb hydrogen until the ratio of hydrogen to metal atoms reaches 2. The hydrides have three phases depending on the degree of hydrogenation. In the dihydride (denoted as the $\gamma$ phase), the metal atoms form a face-centered-cubic (fcc) lattice and the hydrogen atoms occupy the tetrahedral site ($T$ site) formed in the cubic lattice.[3] In hydrides with much lower hydrogen-to-metal ratios (i.e., $x\sim0$), called the $\alpha$ phase, the metal atoms form a body-centered-cubic (bcc) lattice.[4–6] Previous studies of hydrides in the $\alpha$ phase have shown that the hydrogen atoms enter the tetrahedral site and diffuse very quickly in the bcc lattice.[7] In the monohydride (denoted as the $\beta$ phase), which has a bcc lattice, the nature of the hydrogen sites and the dynamical behavior of hydrogen atoms is not clearly understood. The concentration of hydrogen changing the phase from the $\alpha$ to the $\beta$ phase is not known. It is necessary to know the structure of $Ti_{1-y}V_yH_x$ to understand the hydrogen-absorbing properties and the phase relation among the phases. In our previous work, we studied the proton dynamics in the $\beta$ phase using $^1$H NMR through spin-lattice relaxation time ($T_1$) measurements, and the results were interpreted using a local structural model.[8] In this model the local structures of metal atoms around a hydrogen atom were described by a binomial distribution. The hydrogen atoms had different activation energies depending on the local structure of metal atoms, and it was assumed that the hydrogen atoms occupied only the $T$ site.

To study the hydrogen sites and the dynamics in the metal, incoherent inelastic neutron scattering (IINS) measurements have been applied extensively to some metal hydrides.[9–15] Energy transfer corresponding to the local vibrational modes of hydrogen in metal hydrides is observed in the IINS spectra. The excitation energy of the local vibration of a hydrogen atom, $\Delta E$, is described by the following equation:[14]

$$\Delta E(lmn)=E(lmn)-E(000)\ ,$$

where $E(lmn)$ is the perturbed energy of the vibrational state corresponding to the $(lmn)$ harmonic level. $l$, $m$, and $n$ are the quantum numbers for vibrational excitations in each of the three degrees of freedom, respectively. The local vibrational modes of the hydrogen atoms reflect the hydrogen potential, which determines $E(lmn)$, in these systems. The hydrogen potential depends on the chemical and topological environment around a hydrogen atom (i.e., crystal symmetry, hole radius, lattice distortion, and the kinds of host metals).

$TiH_2$ and $VH_{0.33}$, which are the well-known metal hydrides and become the starting point for the discussion of the Ti-V-H system, have been studied in detail.[14] $TiH_2$ has a fcc lattice, in which the hydrogen atom occupies the $T$ site. The local vibrational modes of hydrogen atoms in $TiH_2$ are triply degenerate and they are observed at 147.6 meV at 300 K. The hydrogen potential is described very well by a harmonic potential. On the other hand, $VH_{0.33}$ has a body-centered-tetragonal (bct) lattice, in which the hydrogen atom occupies the octahedral site ($O$ site). In this hydride, the degeneracy of the local vibrational modes is removed, and the in-plane modes are observed at 50 and 57 meV whereas the mode perpendicular to the plane is observed at 220 meV at 30 K. The hydrogen potential is described by a well-like potential

 

(see Fig. 1 in Ref. 14). In the Ti-V-H system, the hydrogen sites, the dynamics, and the potentials are expected to be described as the average of those for $TiH_x$ and $VH_x$.

In this work, we have measured the IINS spectra of the hydrides $\beta$-$Ti_{1-y}V_yH_x$ at 50 K in order to investigate the hydrogen sites and the local structure of metals surrounding the hydrogen atoms. The integral of each peak reflects the fraction of each hydrogen site. A cluster model[16] that considers short-range ordering of either Ti or V is applied to interpret the alloy-composition dependence of the fraction of each hydrogen site, from which we try to estimate the short-range order parameter $\sigma$. The correlation between the arrangements of metal atoms around a hydrogen atom and the types of sites occupied by a hydrogen atom is also discussed.

## II. EXPERIMENT

Titanium powder (purity 99.9%) and vanadium powder (99.9%) were purchased from Soekawa Chemicals Ltd. and High Purity Chemicals Ltd., respectively. The binary alloys $Ti_{1-y}V_y$ were prepared by arc melting of the appropriate mixture of Ti and V powders under an argon atmosphere. The dihydride was prepared according to the procedure described in our previous papers.[3,5] The monohydrides were prepared by the dehydrogenation of the dihydride. The hydrogen concentrations were determined from the volume of hydrogen gas evolved at high temperatures. Four hydrides were prepared; $Ti_{0.1}V_{0.9}H_{0.98}$, $Ti_{0.4}V_{0.6}H_{0.92}$, $Ti_{0.6}V_{0.4}H_{1.1}$, and $Ti_{0.8}V_{0.2}H_{0.94}$. The characterizations such as phase separation and crystal structure were performed by x-ray powder diffraction measurements.

For $Ti_{0.6}V_{0.4}H_{1.1}$ and $Ti_{0.4}V_{0.6}H_{0.92}$, the x-ray powder diffraction gave typical patterns of a bcc structure. All of the reflections observed were able to be assigned to the bcc lattice index. These hydrides consisted of a monophase which was the $\beta$ phase. From the x-ray diffraction results of $Ti_{0.8}V_{0.2}H_{0.94}$ and $Ti_{0.1}V_{0.9}H_{0.98}$, it was inferred that these hydride samples were mixtures of the $\beta$ and $\gamma$ phases of which the unit cell is fcc. The dominant diffraction pattern for $Ti_{0.1}V_{0.9}H_{0.98}$ was found to be body-centered tetragonal,[2] although for $Ti_{0.8}V_{0.2}H_{0.94}$ it was bcc. The fractions of the $\gamma$ phase were estimated to be about 20% in the two hydride samples, and were obtained from the ratio of the intensity of the (200) reflection peak of the fcc lattice to the sum of intensities of the (110) reflection of the bcc lattice and the (200) reflection of the fcc lattice, as listed in Table I. The lattice constants were determined from the x-ray powder diffraction patterns and the results are listed in Table I together with the crystal structure.

We performed IINS measurements using a CAT spectrometer (a crystal analyzer time-of-flight spectrometer)[14,17] which was installed in the neutron scattering facility (KENS) with the pulsed spallation neutron source at the National Laboratory for High Energy Physics (KEK), Japan. The energy resolution of the CAT spectrometer is $\Delta\varepsilon/\varepsilon \sim 2\%$ over a wide energy range of 1–1000 meV. Correction of the peak intensity is necessary to compare the intensities between the peaks observed at the different energy regions, because of the energy distribution of the incident neutron source. The correction of peak intensity is performed by the function $I(\lambda)$ given for this neutron source. The hydrides were wrapped with aluminum foil to make samples ($70\times70\times2$ $mm^3$) and sealed under He gas in an aluminum sample cell ($70\times70\times5$ $mm^3$). The IINS spectra were measured at 50 K and accumulated for 12 h.

## III. RESULTS

The IINS spectra obtained for the four samples at 50 K are shown in Fig. 1. In $Ti_{0.8}V_{0.2}H_{0.94}$, the spectrum consists of two peaks and two shoulders. One peak is relatively narrow and the other is broad; they are located at 13 and 140 meV, respectively. The two broad shoulders appear at 40 and 100 meV. This spectrum has peak positions and intensities similar to that of $TiH_2$, although shoulders are observed and the linewidth of each peak is broader than that for $TiH_2$. In $Ti_{0.6}V_{0.4}H_{1.1}$, the spectrum is similar to that of $Ti_{0.8}V_{0.2}H_{0.94}$, although the peak intensity at 140 meV is weaker than that of $Ti_{0.8}V_{0.2}H_{0.94}$. In $Ti_{0.4}V_{0.6}H_{0.92}$, the spectrum consists of four peaks whose positions are 13, 40, 100, and 140 meV. The peak intensities are comparable to each other except for the peak at the lowest energy. Finally, in $Ti_{0.1}V_{0.9}H_{0.98}$, the spectrum appears to consist of three peaks and one shoulder; peaks at 16, 40, and 145 meV, and a broad shoulder at 110 meV. This spectrum reflects the character of the spectrum of $VH_{0.33}$. The intensities of the peaks located at 40, 100, and 140 meV depend on the alloy compositions. The characteristics of the spectra appear to change gradually from $TiH_2$ to $VH_{0.33}$ through the Ti-V-H system.

TABLE I. Sample characterization of the $Ti_{1-y}V_yH_x$ hydrides from x-ray diffraction and incoherent inelastic neutron scattering.

| Sample $Ti_{1-y}V_yH_x$ | Crystal structure | Lattice const. (Å) | Fraction of $\gamma$ phase (%) x ray | Neutron |
|---|---|---|---|---|
| $Ti_{0.8}V_{0.2}H_{0.94}$ | bcc | 3.33(±0.15) | ~20 | 15 |
| $Ti_{0.6}V_{0.4}H_{1.1}$ | bcc | 3.29(±0.20) | | |
| $Ti_{0.4}V_{0.6}H_{0.92}$ | bcc | 3.23(±0.18) | | |
| $Ti_{0.1}V_{0.9}H_{0.98}$ | bct | 3.04(±0.20) | ~20 | 18 |
| | | 3.38(±0.20) | | |

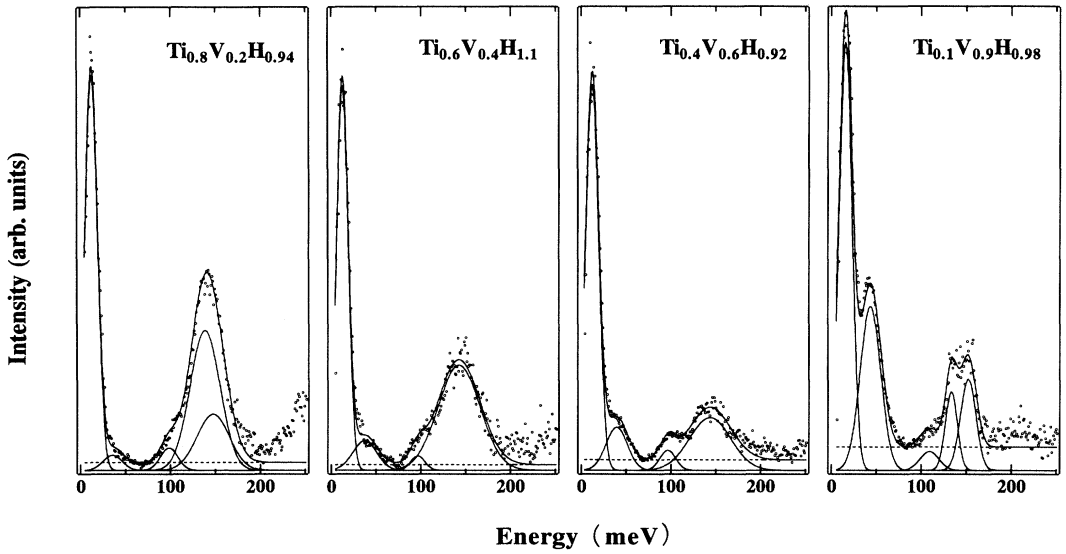


FIG. 1. Incoherent inelastic neutron scattering spectra of $\beta$-$Ti_{1-y}V_yH_x$ ($x \sim 1$; $y = 0.2, 0.4, 0.6, 0.9$) at 50 K. The spectra are normalized by the hydrogen concentrations, the total count, and the energy distribution of incident neutrons. The solid lines are the results of least-squares curve fitting of data with four Gaussians for $y = 0.4$ and 0.6 and with five Gaussians for $y = 0.2$ and 0.9, and the dashed lines are the background noise.

It is necessary to estimate the relative fraction of each peak to discuss the composition dependence of the spectra. The vibration spectra were usually analyzed by superimposing three peaks corresponding to the three degrees of freedom in the normal mode, $\Delta E(100)$, $\Delta E(010)$, and $\Delta E(001)$. In our spectra, it was difficult to analyze using those procedures owing to the weak intensity and the low signal-to-noise ratio. So Gaussian curve fitting of the IINS spectra was used to obtain the integrals of peaks. Four Gaussians were used to fit the IINS spectra of $Ti_{0.4}V_{0.6}H_{0.92}$ and $Ti_{0.6}V_{0.4}H_{1.1}$, but for $Ti_{0.1}V_{0.9}H_{0.98}$ and $Ti_{0.8}V_{0.2}H_{0.94}$ five Gaussians were used. As $Ti_{0.8}V_{0.2}H_{0.94}$ and $Ti_{0.1}V_{0.9}H_{0.98}$ were mixtures of the $\beta$ and $\gamma$ phases, the extra Gaussian was necessary for these two hydrides to take account of the contribution from the $\gamma$ phase, which was expected to give an IINS peak around 145 meV by analogy with $TiH_2$. The results of the least-squares fitting are shown in Fig. 1 with solid lines and the parameters obtained by the data fitting are listed in Table II.

TABLE II. The peak energies, the linewidths $\Gamma$, and the relative intensity of the vibrational modes of the hydrogen atom and the metal lattice in Ti-V alloys, and the fraction of the corresponding hydrogen site.

| Sample | Peak (meV) | $\Gamma$ (meV) | Intensity $I/I_{max}$ | Fraction (%) |
|---|---|---|---|---|
| $Ti_{0.8}V_{0.2}H_{0.94}$ | 13±1 | 9.7±0.2 | 1.0 | |
| | 36±3 | 14.8±1.0 | 0.04±0.01 | 8.6 |
| | 99±3 | 13.6±1.0 | 0.06±0.01 | 7.6 |
| | 139±3 | 23.4±0.5 | 0.35±0.02 | 83.8 |
| | 148±2[a] | 25.2±0.5 | 0.14±0.02 | |
| $Ti_{0.6}V_{0.4}H_{1.1}$ | 13±1 | 8.9±0.3 | 1.0 | |
| | 38±3 | 18.7±1.0 | 0.08±0.01 | 19.3 |
| | 97±2 | 11.0±1.0 | 0.04±0.01 | 3.7 |
| | 143±2 | 33.1±0.5 | 0.27±0.02 | 77.0 |
| $Ti_{0.4}V_{0.6}H_{0.92}$ | 13±1 | 10.1±0.2 | 1.0 | |
| | 40±1 | 16.7±0.5 | 0.11±0.01 | 35.7 |
| | 97±2 | 12.4±0.5 | 0.05±0.01 | 8.1 |
| | 144±2 | 32.2±1.0 | 0.14±0.01 | 56.2 |
| $Ti_{0.1}V_{0.9}H_{0.98}$ | 16±1 | 10.1±0.2 | 1.0 | |
| | 44±1 | 16.1±0.2 | 0.38±0.01 | 93.6 |
| | 110±3 | 14.7±1.0 | 0.04±0.01 | 6.4 |
| | 134±3[a] | 9.3±0.5 | 0.18±0.02 | |
| | 152±3[a] | 12.0±0.5 | 0.21±0.03 | |

[a]This peak is assumed to originate from the $\gamma$ phase.

## IV. ANALYSIS AND DISCUSSION

### A. Peak assignments of IINS spectra

The peak observed at the lowest energy, which is 13 meV for $Ti_{0.8}V_{0.2}H_{0.94}$, $Ti_{0.6}V_{0.4}H_{1.1}$, and $Ti_{0.4}V_{0.6}H_{0.92}$ and 16 meV for $Ti_{0.1}V_{0.9}H_{0.99}$, is known to be the acoustic branch of the metal lattice vibrational mode in the crystal,[10] and will be neglected in the following discussion. The other peak intensity ratios depend on the Ti content, as shown in Fig. 1. This suggests that the observed peaks result from the local vibrational modes of three types of hydrogen sites. As described in the Introduction, we refer to $TiH_2$ and $VH_{0.33}$ to assign the observed peaks to the corresponding hydrogen sites. The excitation energies $\Delta E(100)$, $\Delta E(010)$, and $\Delta E(001)$ of a hydrogen atom occupying the $O$ site in $VH_{0.33}$ were 50, 57, and 220 meV.[14] The excitation energy of a hydrogen atom occupying the $T$ site in $TiH_2$ was 147.6 meV.[14] By comparing the observed spectra with the reported work, the peaks observed at $36 \leq \varepsilon \leq 44$ meV are considered to be assigned to the in-plane local vibrational modes of a hydrogen atom occupying the $O$ site, and those at $134 \leq \varepsilon \leq 152$ meV to the local vibrational modes of hydrogen atoms occupying the $T$ site. Although the local vibrational mode for the motion perpendicular to the in-plane motion at the $O$ site is observed at 220 meV in $VH_{0.33}$, the intensity and the signal-to-noise ratio in our spectra are not good enough to discuss this mode. Thus this mode is omitted from the following discussion. The peak at $97 \leq \varepsilon \leq 110$ meV is located at an intermediate energy range between those of the $O$ and $T$ sites. In fact, Hempelmann *et al.* observed a well-defined peak at a similar energy region (about 108 meV) for $ZrV_2H_{4.5}$, which was assigned to a hydrogen atom occupying the $V_4$ site.[18] The crystal structure of $ZrV_2H_{4.5}$ is different from that of our system, but the local structures around a hydrogen atom are considered to be similar between the two cases. So we refer to their work to assign the peak at this energy range to the $T$ site consisting of V atoms. The hydrogen sites corresponding to the three peaks are denoted as the $T_1$, $T_2$, and $O$ sites from the higher-energy range, respectively, in the following discussion.

Before we discuss the composition dependence of the IINS spectra, we perform a correction for the coexistence of the $\gamma$ phase in $Ti_{0.1}V_{0.9}H_{0.92}$ and $Ti_{0.8}V_{0.2}H_{0.94}$. Assuming that the two peaks observed at 134 and 152 meV for $Ti_{0.1}V_{0.9}H_{0.98}$ and the peak observed at 148 meV for $Ti_{0.8}V_{0.2}H_{0.94}$ result from the $\gamma$ phase, the fractions of the $\gamma$ phase obtained from neutron scattering are consistent with those from x-ray diffraction as explained below. The peak integrals of the $\gamma$ phase are about 30% and 27%, respectively, of the total integrals of peaks, if the peak at the lowest energy is excluded. To estimate the fraction of the $\gamma$ phase in the metal atom base we consider the ratio of the hydrogen contents in the $\beta$ and $\gamma$ phases. For example, the ratio of the $\beta$ and $\gamma$ phases in the metal atom base is 70:(30/2) in $Ti_{0.1}V_{0.9}H_{0.92}$ because the hydrogen-to-metal ratios in the $\beta$ and $\gamma$ phases are 1 and 2, respectively. Consequently, the fractions of the $\gamma$ phase for $Ti_{0.1}V_{0.9}H_{0.92}$ and $Ti_{0.8}V_{0.2}H_{0.94}$ are 18% and 15%, respectively, which agree with those estimated from x-ray diffraction (see Table I).

Excluding the contributions from the $\gamma$ phase and the metal lattice vibration, the spectra consist of at most three peaks. Their intensities and positions change with the metal composition of the alloy. The relative intensity of the peak corresponding to the hydrogen atom occupying the $O$ site decreases and the peak position shifts slightly to lower energies, with increasing Ti content in the alloys. In general, the vibrational energy is proportional to the inverse of the metal-hydrogen distance as a first approximation. So this variation of the peak position is considered to be due to the lattice expansion caused by Ti incorporation. The energy range in this system is lower than the expected position, which is about 45 meV estimated using the lattice constants $a = 3.0$ Å for $VH_{0.33}$ and 3.33 Å for $Ti_{0.8}V_{0.2}H_{0.94}$. Perturbations such as the shape change of the hydrogen potential might cause this shift to lower energy. For the peaks corresponding to the $T_2$ site the relative peak intensity is approximately constant and the peak position is constant within the experimental error except for $Ti_{0.1}V_{0.9}H_{0.98}$. The peak position 110 meV for $Ti_{0.1}V_{0.9}H_{0.98}$ is greater by 10 meV than those of the other hydrides. We consider that this shift is caused by the difference in the crystal structure. For the peaks corresponding to the $T_1$ site the relative peak intensity increases with increasing Ti content in the alloys and the peak position is constant within the experimental error.

The linewidths $\Gamma$ in Table II are relatively broad compared with those of other pure metal hydrides such as $TiH_2$, $VH_{0.33}$,[14] and $ZrV_2H_x$,[18] because three degrees of freedom for the local modes for the $T$ site and two for the $O$ site are approximated by a Gaussian curve. In addition, the distribution of the lattice constants due to the formation of the disordered alloys causes further broadening.

### B. Composition dependence of the fraction of each hydrogen site

The composition dependence of the hydrogen sites is analyzed in terms of only the fraction of each site in the hydrides due to the difficulty in determining the absolute values. The $O$ and $T$ sites have two and three degrees of freedom for vibrational excitation, respectively. The peak integrals were corrected for the degeneracy of the vibrational modes; 2 and 3 for the $O$ and $T$ sites, respectively. The ratio of the corrected integrals gives the fraction of the hydrogen site in the Ti-V alloys. The fractions of the three kinds of hydrogen sites are listed in Table II and are plotted against the fraction of Ti atoms, $1-y$, in Fig. 2. The fraction of the $T_1$ site increases and that of the $O$ site decreases with increasing Ti content. The fractions of the two sites become comparable when the Ti content equals 0.4. These fractions change monotonically but not linearly with the Ti content, whereas the fraction of the $T_2$ site is constant within the experimental error. The fraction of the latter site is smaller than those of the other two sites. These results show that the types and the number of the hydrogen sites are strongly correlated with

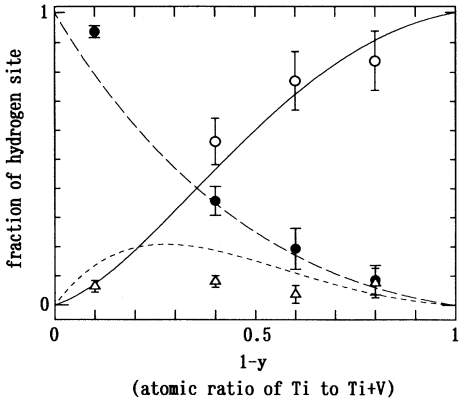


FIG. 2. Composition dependence of the fractions of the hydrogen site. The fractions of the hydrogen site for the $O$ site (●), $T_1$ site (○), and $T_2$ site (△) are plotted against the fraction of Ti (i.e., $1-y$). The degeneracies of the local vibrational modes of the hydrogen atom are taken into account to convert the peak integrals to the fractions of the hydrogen sites. The lines were calculated values using Eq. (5) with $\sigma=0.43$, $n=4$, and $m=5$. For $Ti_{0.1}V_{0.9}H_{0.98}$, the fraction of the $T_1$ site arising from the $\beta$ phase is too small to be estimated.

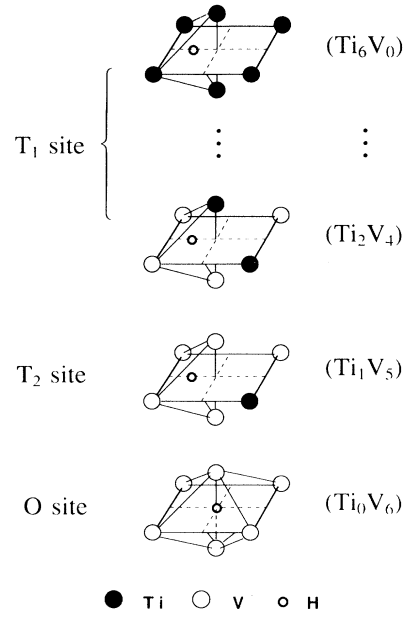


FIG. 3. Schematic description of the correlation between the arrangement of metals and the hydrogen site in the cluster. This scheme corresponds to the case of $n=4$ and $m=5$; the hydrogen atom occupies the $T_1$ site in the clusters from $Ti_6V_0$ to $Ti_2V_4$, the $T_2$ site in $Ti_1V_5$, and the $O$ site in $Ti_0V_6$.

the composition of the host alloys.

These variations of the hydrogen-site fractions are discussed in terms of clusters, which form octahedra surrounding the hydrogen atom [i.e., $Ti_{6-i}V_i$ $(i=0-6)$]. We consider a model of hydrogen sites in the clusters, making reference to the hydrogen sites in pure metal hydrides such as $VH_{0.33}$ and $TiH_2$. This model is schematically shown in Fig. 3. The hydrogen atoms in the pure metal hydrides composed of only V or Ti occupy the $O$ or $T$ sites, respectively.[7] The octahedron in $VH_{0.33}$ is composed of only V atoms and represented by $Ti_0V_6$, whereas in $TiH_2$ it is composed of Ti and represented by $Ti_6V_0$. In our system, the octahedra are composed of Ti and V and show the seven kinds of configurations from $Ti_6V_0$ to $Ti_0V_6$. If the stability of the hydrogen site is determined by the metal-hydrogen interaction as a first approximation, the hydrogen atoms at the tetrahedral sites are stable at the Ti-rich content and the hydrogen atoms at the octahedral sites are stable at the V-rich content. Also, the affinity of Ti to the hydrogen atom is generally greater than that of V.[19,20] Taking into account the difference in the affinity of metal to hydrogen between Ti and V, we propose a scheme for the hydrogen site in the cluster. When the configuration of the cluster changes from $Ti_6V_0$ to $Ti_0V_6$, the hydrogen site changes from the $T_1$ site to the $O$ site through the occupation of the $T_2$ site. The boundaries between the sites will be estimated in the next section.

### C. Cluster model

We consider a cluster composed of two species and having the form $Ti_{6-i}V_i$. The fractions of $Ti_{6-i}V_i$, $p(i)$, are given by the binomial distribution in the case of a random distribution of Ti and V in the $Ti_{1-y}V_y$ disordered alloys. In the cluster model proposed by Brouwer and co-workers,[16] the inclination of the distribution in the fractions is described using a short-range order parameter $\sigma$. $\sigma$ is zero for a random distribution of metal atoms, and is defined by the following pair probabilities (with $p_{Ti}=1-y$ and $p_V=y$):[21,22]

$$p_{TiTi}=p_{Ti}+(1-p_{Ti})\sigma \ , \tag{1a}$$

$$p_{TiV}=p_V-p_V\sigma \ , \tag{1b}$$

where $p_{TiTi}$ is the probability to find a Ti atom as nearest neighbor of the first Ti atom and $p_{TiV}$ is the probability to find a V atom as nearest neighbor of the first Ti atom. The pair probabilities are related to one another by

$$p_{TiTi}+p_{TiV}=1 \ , \tag{2a}$$

$$p_{Ti}p_{TiV}-p_Vp_{VTi}=0 \ . \tag{2b}$$

(Relations for $p_{VTi}$ and $p_{VV}$ are obtained by exchanging Ti and V in the above equations.)

We consider the physical meaning of the parameter $\sigma$. For $\sigma>0$ both Ti and V atoms prefer to form clusters of Ti or V atoms, while for $\sigma<0$ both Ti and V atoms form ordered structures. That is, in the $Ti_{1-y}V_y$ alloy complete ordering occurs for $\sigma=-1$. Phase separation occurs for $\sigma=1$ and $Ti_{6-i}V_i$ $(i=1-5)$ clusters vanish.

The cluster model (for $\sigma>0$) incorporates all 12 bonds found in an octahedron. Consider, for example, a $Ti_6V_0$ cluster. The probabilities to find the first and second Ti atoms are simply $p_{Ti}$ and $p_{TiTi}(\sigma)$, respectively. $\sigma$ may be viewed as an interpolation for $p_{TiTi}(\sigma)$ between $p_{Ti}$ and 1. Consider a third Ti atom placed in the cluster. The probability for this third atom, $p_{TiTiTi}(\sigma)$, must be at

least $p_{\mathrm{TiTi}}(\sigma)$ and at most 1. Extending Eq. (1a) we get

$$p_{\mathrm{TiTiTi}}=p_{\mathrm{TiTi}}+(1-p_{\mathrm{TiTi}})\sigma \tag{3}$$

and the probabilities from the fourth to the sixth Ti atoms are similarly derived. The probability to find a $Ti_6V_0$ cluster in the alloy is given by

$$p(i=0,\sigma)=p_{\mathrm{Ti}}p_{\mathrm{TiTi}}p_{\mathrm{TiTiTi}}p_{\mathrm{TiTiTiTi}}p_{\mathrm{TiTiTiTi}} \times p_{\mathrm{TiTiTiTiTi}}p_{\mathrm{TiTiTiTiTiTi}} \cdot \tag{4}$$

Calculations for other clusters were given elsewhere.[16]

The hydrogen-site fractions are given by allocating each fraction of the clusters to the $T_1$, $T_2$, and $O$ sites as follows:

$$P_{T_1}(\sigma)=\sum_{i=0}^{n} p(i,\sigma) , \tag{5a}$$

$$P_{T_2}(\sigma)=\sum_{i=n+1}^{m} p(i,\sigma) , \tag{5b}$$

$$P_{O}(\sigma)=\sum_{i=m+1}^{6} p(i,\sigma) , \tag{5c}$$

where $n$ and $m$ are adjustable parameters representing the border numbers between the $T_1$ and $T_2$ sites and between the $T_2$ and $O$ sites, respectively. Parameters $n$ and $m$ must be integers satisfying the conditions $0\le n<m<6$. Thus, in this model, the parameter $\sigma$ represents the degree of the clustering of metal atoms, and $n$ and $m$ determine the kinds of sites where the hydrogen atom enters.

Figure 4 shows site fractions calculated by using Eq. (5) for various values of adjustable parameters $\sigma$, $n$, and $m$ to demonstrate the dependence of the calculated site fractions on the parameters. The $O$-site fraction has a linear relation with the Ti content at $\sigma=1$. When the parameters $n$ and $m$ are constant and $\sigma$ changes from 1 to 0, the curve for the $O$ site is no longer linear, as shown in Fig. 4(a). The fraction of the $T_2$ site is zero at $\sigma=1$, and increases as $\sigma$ changes from 1 to 0 [Fig. 4(b)]. It reaches a maximum at $1-y=0.5$ for a given value of $\sigma$ at $n=2$ and $m=3$. The curve of the $O$ site and the maximum of the curve of the $T_2$ site shift from low-concentration side of Ti to the high-concentration side with decreasing $n$ and $m$, when $\sigma$ is constant [Figs. 4(c) and 4(d)]. By regressing Eq. (5) onto the data we obtained $\sigma=0.43\pm0.05$, $n=4$, and $m=5$. The calculated fractions are shown in Fig. 2 together with the experimental data.

### D. Clustering in Ti-V alloy

The $\sigma$ value obtained is compared with literature values,[16] which were estimated by Brouwer *et al.* from the activation energy for diffusion and the enthalpies of solution for hydrogen in various $Ti_{1-y}V_y$ alloys.[23–26] The range of $\sigma$ in the literature is $0.36\le\sigma\le0.51$. There are two possible origins to cause the differences in $\sigma$; the

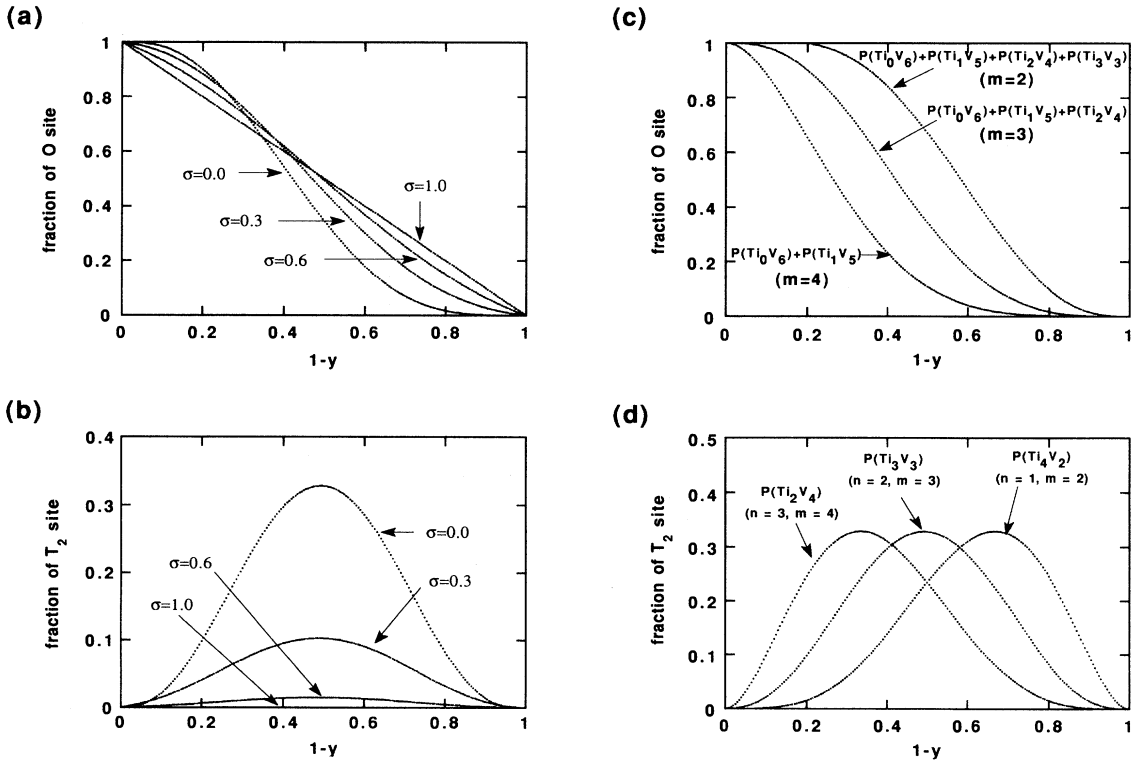


FIG. 4. Simulations of the fractions for the $O$ and $T_2$ sites. The short-range order parameter ($\sigma$) dependences of the $O$-site (a) and $T_2$-site (b) fractions were calculated using Eq. (5) with $n=2$ and $m=3$. The dependences of the $O$-site (c) and $T_2$-site (d) fractions on $n$ and $m$ were calculated with $\sigma=0$.

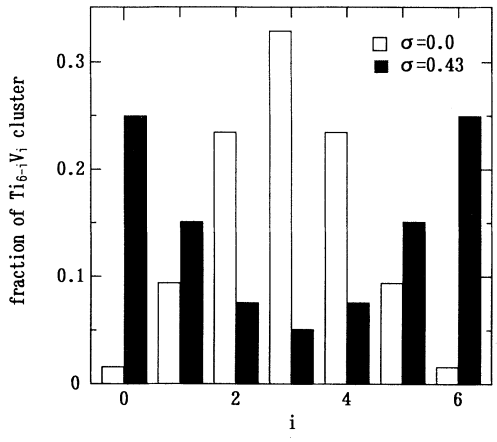


FIG. 5. Fractions of the $Ti_{6-i}V_i$ clusters in the $Ti_{0.5}V_{0.5}$ alloy at two given values of $\sigma$.

first is conditions of synthesis and thermal treatment such as annealing temperature, and the second is the hydrogen concentrations in the Ti-V alloys. In addition, our cluster model derived above might be too simple to describe the actual local structure in the alloy. In an actual system a hydrogen atom occupying a site will block a hydrogen atom from entering in the nearest-neighbor empty sites (selective blocking), and the site occupancies of hydrogen atoms depend on the temperature because of the differences in the site energy among the three sites. However, the $\sigma$ value obtained in this work is in good agreement with literature values in spite of the simplified model. These $\sigma$ values might be an intrinsic value for the Ti-V alloy system.

The short-range order parameter $\sigma=0.43\pm0.05$ shows clustering of either Ti or V in the alloys. The fractions of the $Ti_{6-i}V_i$ clusters in the $Ti_{0.5}V_{0.5}$ alloy are calculated for $\sigma=0$ and 0.43 and the results are shown in Fig. 5. For $\sigma=0.43$ the fractions of $Ti_2V_4$, $Ti_3V_3$, and $Ti_4V_2$ decrease while those of $Ti_0V_6$, $Ti_1V_5$, $Ti_5V_1$, and $Ti_6V_0$ increase, when compared with those for $\sigma=0$ (the binominal distribution). The fraction of $Ti_3V_3$ becomes one-sixth and the fractions of $Ti_2V_4$ and $Ti_4V_2$ become one-third. The fractions of $Ti_1V_5$ and $Ti_5V_1$ are about two times greater, and those of $Ti_0V_6$ and $Ti_6V_0$ are about ten times greater. These considerations show that Ti and V atoms are easy to aggregate around the same kinds of metals. It is possible to make Ti-V alloys with any composition, and the alloys appear to be homogeneous macroscopically. However, there is a large inclination of the distribution of the metal atoms microscopically.

## V. CONCLUSION

The types of hydrogen sites in $\beta$-$Ti_{1-y}V_yH_x$ are revealed by means of incoherent inelastic neutron scattering measurements. The peaks for hydrogen atoms occupying different sites are observed in the energy ranges $36\leq\varepsilon\leq44$ meV, $97\leq\varepsilon\leq110$ meV, and $134\leq\varepsilon\leq152$ meV, and the intensities depend on the composition of the alloys. These peaks are assigned to the hydrogen atoms occupying the octahedral site, the tetrahedral site consisting of only V atoms ($V_4$ site), and the other tetrahedral site, respectively. The composition dependence of the fractions of the hydrogen sites is analyzed by a cluster model incorporating the short-range ordering of metals. As a result of the analysis, we obtain the short-range order parameter $\sigma=0.43\pm0.05$.

## ACKNOWLEDGMENTS

The authors wish to thank Dr. E. Akiba, K. Nomura, Y. Ishido, and Dr. H. Hayakawa for synthesis of the dihydrides and for the use of the x-ray diffractometer.

[1]H. Nagel and R. S. Perkins, Z. Metallkd. **66**, 362 (1975).
[2]S. Ono, K. Nomura, and Y. Ikeda, J. Less-Common Met. **72**, 159 (1983).
[3]S. Hayashi, K. Hayamizu, and O. Yamamoto, J. Less-Common Met. **113**, 1 (1987).
[4]B. Nowak, Y. Chabre, and R. Andreani, J. Less-Common Met. **130**, 193 (1987).
[5]B. Nowak, S. Hayashi, K. Hayamizu, and O. Yamamoto, J. Less-Common Met. **123**, 75 (1986).
[6]S. Hayashi and K. Hayamizu, J. Less-Common Met. **161**, 61 (1990).
[7]T. Schober and H. Wenzl, in *Hydrogen in Metals II,* edited by G. Alfled and J. Völkl (Springer-Verlag, Berlin, 1978), p. 11.
[8]T. Ueda, S. Hayashi, and K. Hayamizu, Phys. Rev. B **48**, 5837 (1993).
[9]T. Springer, Z. Phys. Chem. B **115**, S141 (1979).
[10]V. A. Semenov and Yu. V. Lisichkin, Sov. Phys. Solid State **24**, 2037 (1982).
[11]J. Eckert, J. A. Goldstone, D. Tonks, and D. Richter, Phys. Rev. B **27**, 1980 (1983).
[12]A. Magerl, J. J. Rush, J. M. Rowe, D. Richter, and H. Wipf, Phys. Rev. B **27**, 927 (1983).
[13]A. Magerl, J. J. Rush, and J. M. Rowe, Phys. Rev. B **33**, 2093 (1986).
[14]S. Ikeda and N. Watanabe, J. Phys. Soc. Jpn. **56**, 565 (1987).
[15]I. S. Anderson, N. F. Berk, J. J. Rush, and T.-J. Udovic, Phys. Rev. B **37**, 4358 (1988).
[16]R. C. Brouwer, J. Rector, N. Koeman, and R. Griessen, Phys. Rev. B **40**, 3546 (1989).
[17]S. Ikdea and N. Watanabe, Nucl. Instrum. Methods Phys. Res. Sect. A **221**, 571 (1984).
[18]R. Hempelmann, D. Richter, O. Hartmann, E. Karlsson, and R. Wäppling, J. Chem. Phys. **90**, 1935 (1989).
[19]O. J. Kleppa, P. Dantzer, and M. E. Melnichak, J. Chem. Phys. **61**, 4048 (1974).
[20]P. Dantzer, O. J. Kleppa, and M. E. Melnichak, J. Chem. Phys. **64**, 139 (1976).
[21]P. Eisenberger and B. Lengeler, Phys. Rev. B **22**, 3551 (1980).
[22]D. Nguyen Manh, D. Mayou, A. Pasturel, and F. Cyrot-Lackman, J. Phys. F **15**, 1911 (1985).
[23]S. Tanaka and H. Kimura, Trans. Jpn. Inst. Met. **20**, 647 (1979).
[24]D. J. Pine and R. M. Cotts, Phys. Rev. B **28**, 641 (1983).
[25]P. S. Rudman, Acta Metall. **12**, 1381 (1964).
[26]D. T. Peterson and S. O. Nelson, Metall. Trans. **16A**, 367 (1985).